Sidlab Co

dimension

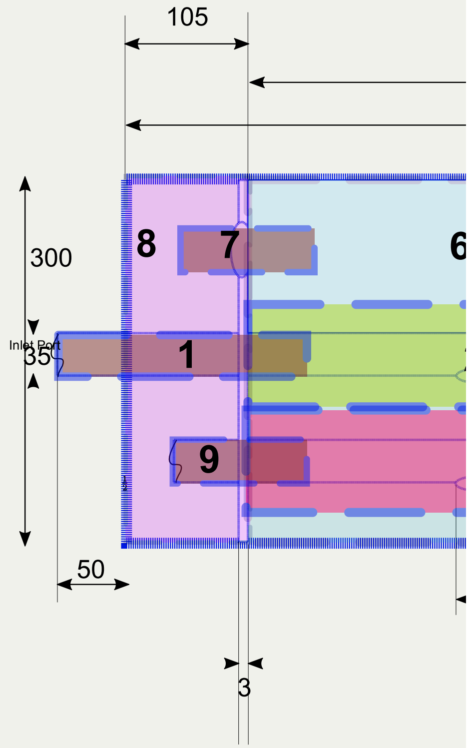


16

le Download Center

Multichamber

Michael Raba, MSc Candida

Created: 2025-0

ANSYS Simulation

- **File:** `Mark-I-MDF-clearned-data.wbpz`
- **Created with:** ANSYS 2023 R2
- ⬇ **Download ANSYS File**

Sidlab and Ansys Fi

Muffler System

ıte at University of Kentucky

9-15 Mon 12:38

SIDLAB Model

- **File:** `Mark3Sid.zip`
- **Created with:** SIDLAB 5.1
- **⬇ Download SIDLAB File**

s (0–1000 Hz) Simlab model

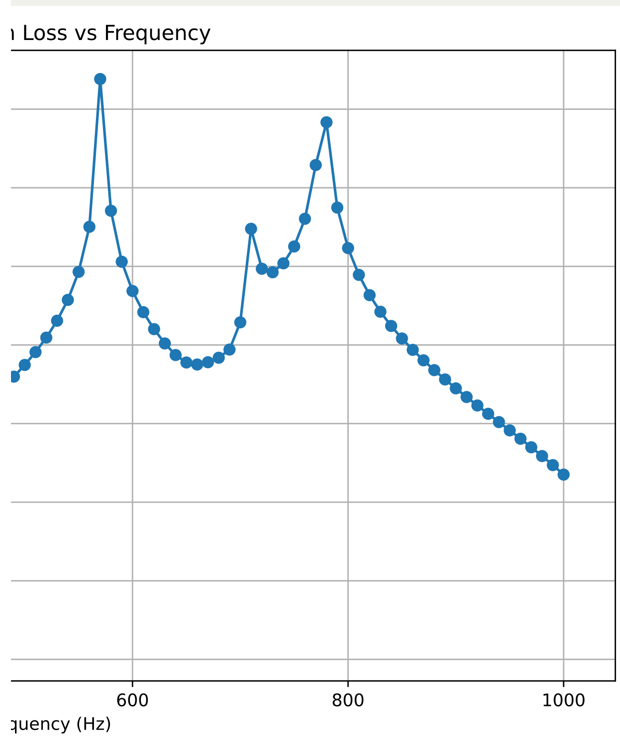

# Simlab S?ler Internal Geometry

Simulated Transmission Los

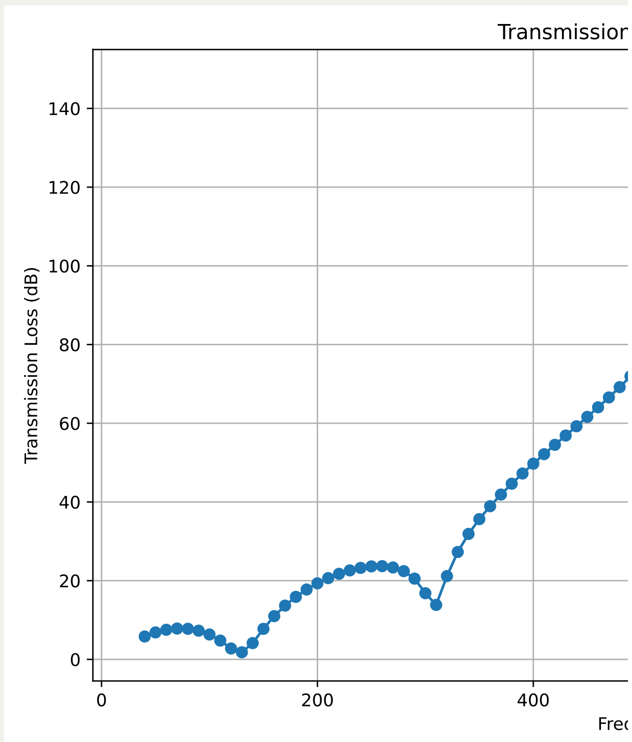


12

mulation

Dime

pproximating muffler walls as fluid at 20 deg C

dimension

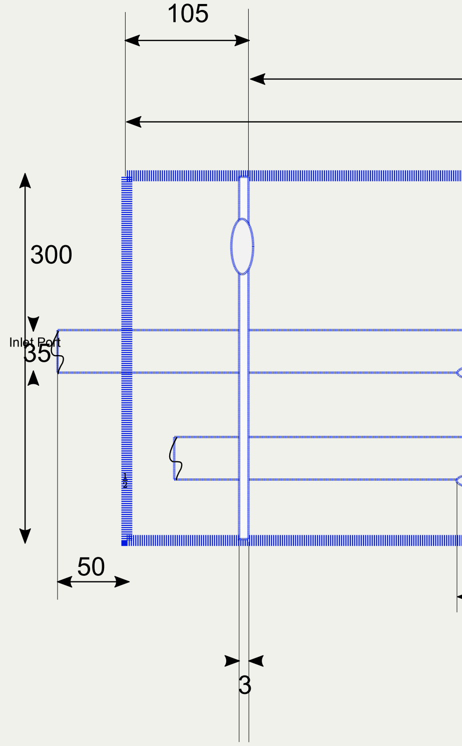


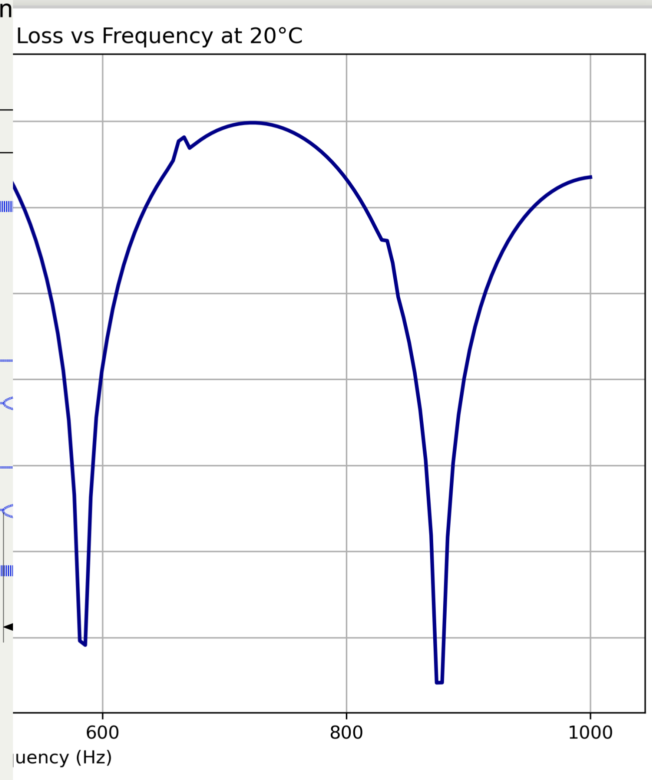


6

uffler between 5 Hz and 1000 Hz at 20°C.

Ansys Si

Simulated Transmission Loss (0–1000 Hz) by a nsions

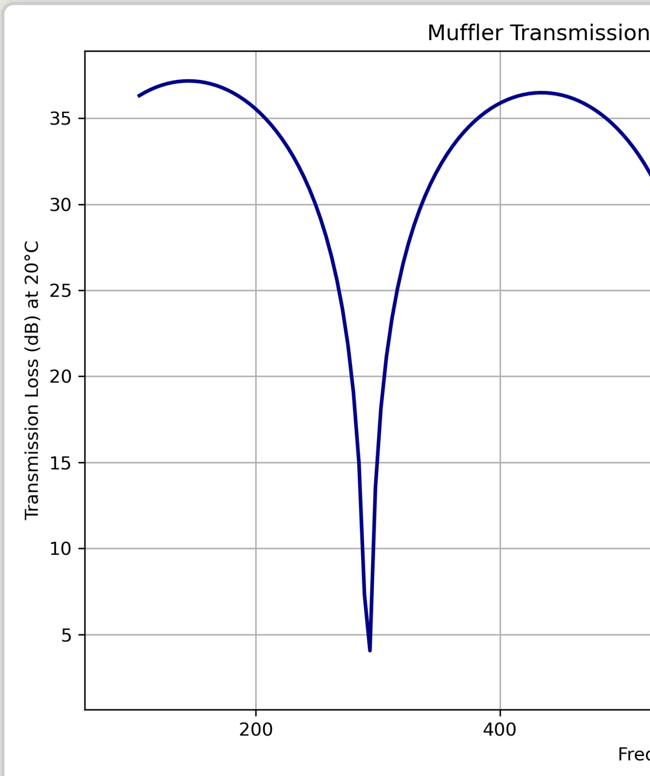


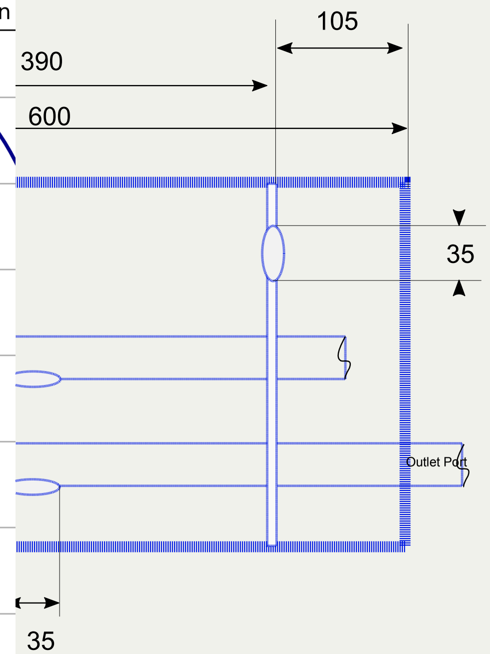


**Figure:** Transmission Loss curve of the m

10

## Schematic Variants for Muffler Subcomponents

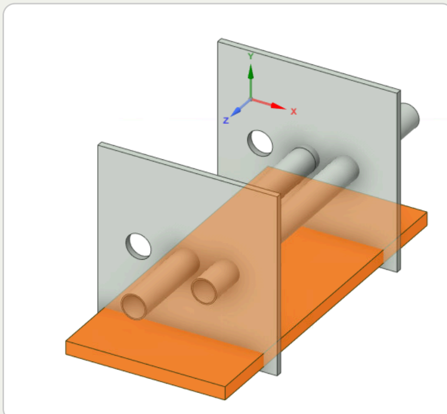

Part 1 — Chamber and Baffle

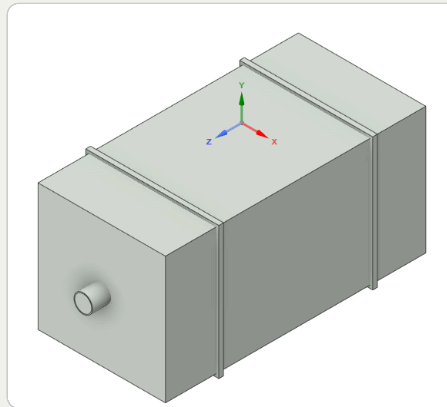

Part 2 — Fluid domain

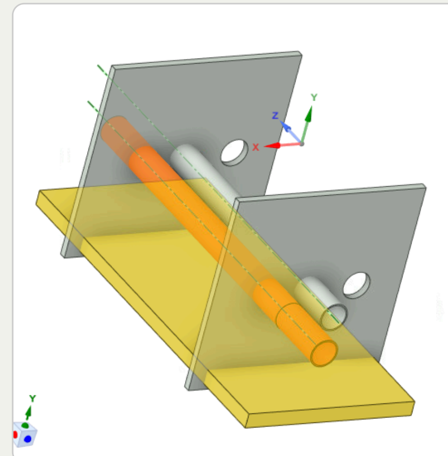

Part 3 — Fiberglass Absorbant (gold)

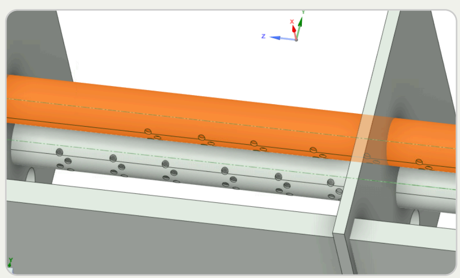

Part 4 — Showing perforates (aimed at fiberglass)

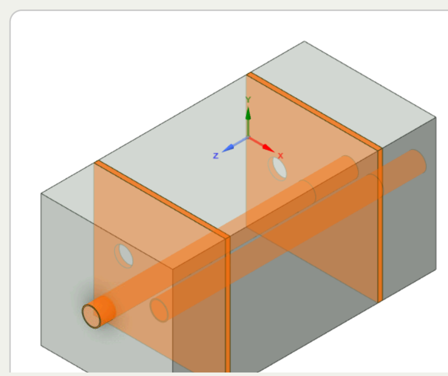

Part 5 — Final Assembly View

mponents

al units in mm

Anand Viscoplasticity (

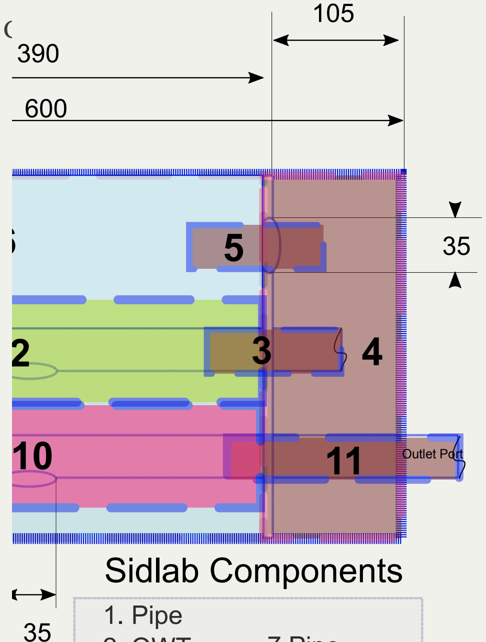


Sidlab Components

1. Pipe
2. QWT
3. Pipe
4. QWT
5. Pipe
6. QWT
7. Pipe
8. QWT
9. Pipe
10. QWT
11. Pipe

**Image Reference**

Values are from correspond to 60Sn40Pb solder parameters used in Anand's model:

- $S_0$: Initial deformation resistance
- $Q/R$: Activation energy over gas constant
- $A$: Pre-exponential factor for flow rate
- $\xi$: Multiplier of stress inside sinh
- $m$: Strain rate sensitivity of stress
- $h_0$: Hardening/softening constant
- $\hat{s}$: Coefficient for saturation stress
- $n$: Strain rate sensitivity of saturation
- $a$: Strain rate sensitivity of hardening or softening

# Simulated vs Measıand-Type Viscoplastic Model

## Measured vs Simulated TL

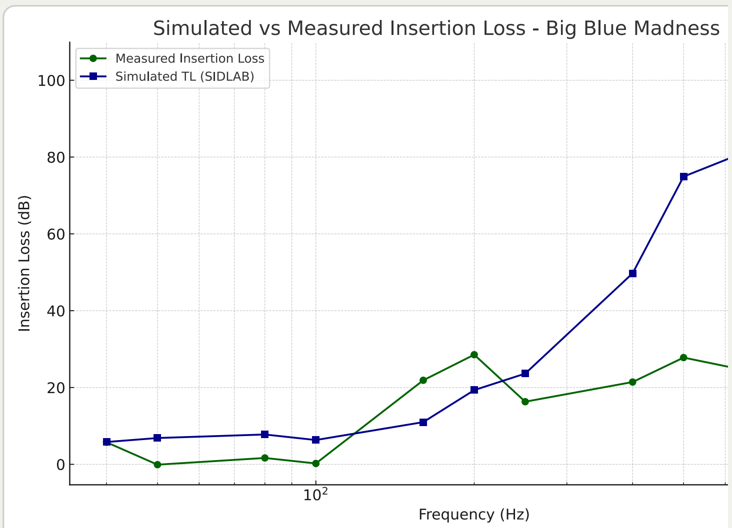


### Evolution of Deformation Resistance $s$

- $$\dot{s} = h_0 \left|1 - \frac{s}{s^*}\right|^a \text{sign}\left(1 - \frac{s}{s^*}\right) \dot{\varepsilon}^p$$
- Describes dynamic hardening and softening of the material.
- $s$ evolves depending on proximity to $s^*$ and flow activity.

Note: Constants $A, Q, m, j, h_0, \hat{s}, n, a$ are material-specific and fitted to experimental creep/strain rate data.

Main Equations of Wang's Anured Insertion Loss

## Flow Rule (Plastic Strain Rate)

- $$\dot{\varepsilon}^p = A\exp\left(-\frac{Q}{RT}\right)\left[\sinh\left(\frac{j\sigma}{s}\right)\right]^{1/m}$$
- Plastic strain rate increases with stress and temperature.
- No explicit yield surface; flow occurs at all nonzero stresses.

## Deformation Resistance Saturation $s^*$

- $$s^* = \hat{s}\left(\frac{\dot{\varepsilon}^p}{A}\exp\left(\frac{Q}{RT}\right)\right)^n$$
- Defines the steady-state value that $s$ evolves toward.
- Depends on strain rate and temperature.

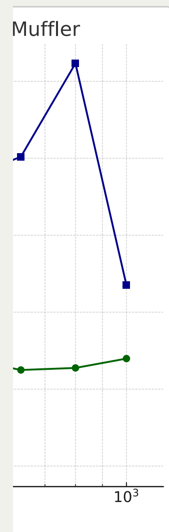


## Insertion Loss Explanation

Insertion Loss (IL) quantifies how much sound is attenuated when a muffler is added to the system.

**General formula:**

$$\mathrm{IL} = 10\log_{10}\left(\frac{P_{\text{baseline}}}{P_{\text{muffler}}}\right)$$

Because our data is already in decibels (dB), this simplifies to:

$$\mathrm{IL} = \text{Power}_{\text{baseline (dB)}} - \text{Power}_{\text{muffler (dB)}}$$

Refer

Cited


1. Munjal ML. *Acoustics of Ducts and Mufflers*. 2nd ed. V
https://doi.org/10.1002/9781118443125
2. Dokumacı E. *Duct Acoustics: Fundamentals and Appli*
Press; 2021. ISBN: 9781108840750. https://doi.org/10


**Note:** These references are foundational texts in muffler a
schematic development, an





**Key Insights from Wang (2001)**

- "At lower strain rates, recovery dominates… the stress levels off early."
- "At high strain rates, hardening dominates, and the stress grows continuously."

Anand's model smoothly captures strain-rate and temperature dependence of solder materials.

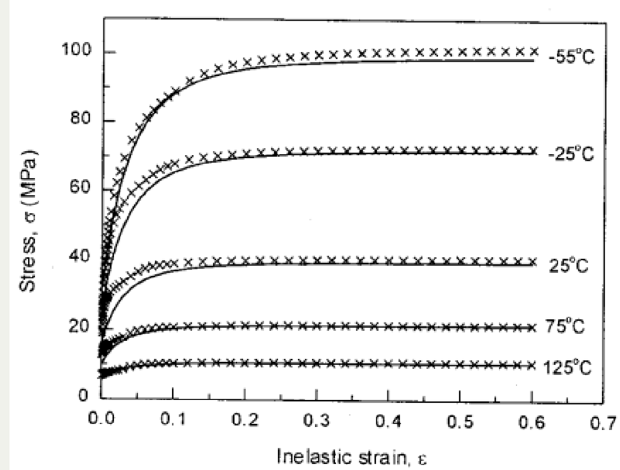


(b) $\dot{\varepsilon}=1.0\times10^{-4}\ s^{-1}$

## Comparing Anand Model Pr

### Observed Behavior

- **Top Graph (a):** $\dot{\varepsilon} = 10^{-2}\,\mathrm{s}^{-1}$
- High strain rate → higher stress
- Recovery negligible → pronounced hardening
- **Bottom Graph (b):** $\dot{\varepsilon} = 10^{-4}\,\mathrm{s}^{-1}$
- Lower strain rate → lower stress at same strain
- Recovery and creep effects more significant

**Model Accuracy:** Lines = model prediction, X = experimental data

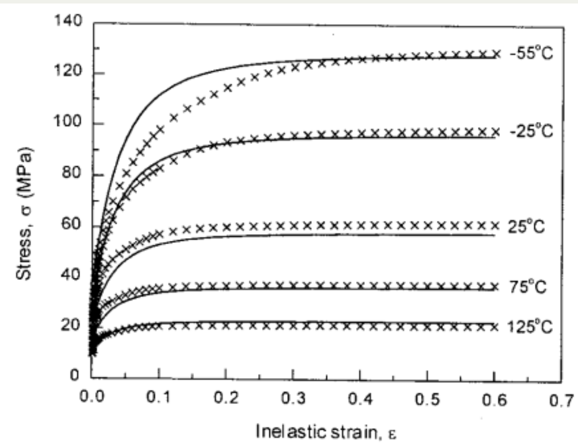


(a) $\dot{\varepsilon} = 1.0\times10^{-2}\,\mathrm{s}^{-1}$

28

ences

Works

Viley; 2014. ISBN: 9781118443125.

cations to Mufflers and Silencers*. Cambridge University

.1017/9781108840750

nd duct acoustics and were consulted for system modeling,
d transmission loss analysis.

# Anand Model: Viscoelastoplasticity

Michael Raba, MSc Candida

Created: 2025-0



001) Apply to Solder

## Why Wang's Paper Matters

ıand's unified viscoplastic framework to model solder behavior.
ıodel can be reduced and fitted from experiments.
:he theory into engineering-scale implementation.
ılder joints in microelectronic packages (chip on PCB, soldered
ıs).

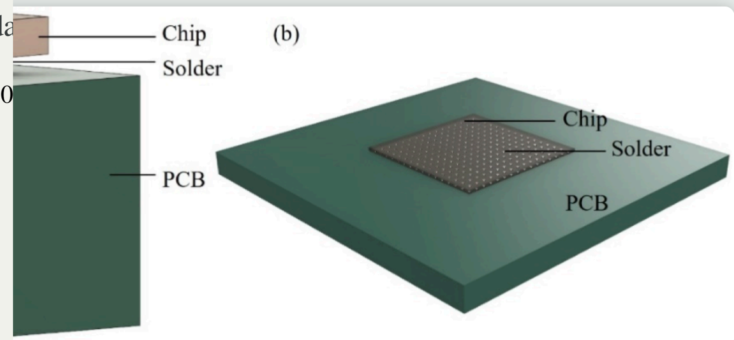

Case Study: Wang (2

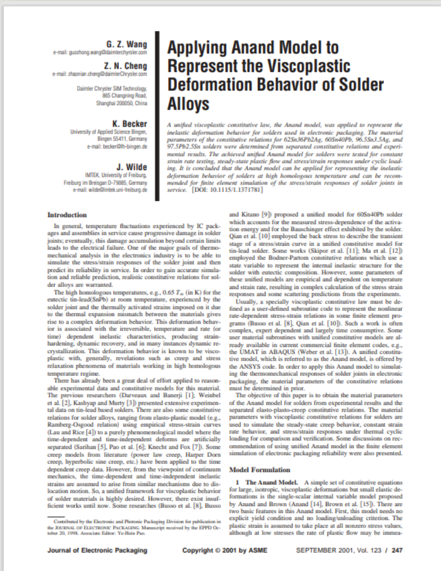
G. Z. Wang
Z. N. Cheng
K. Becker
J. Wilde

## Applying Anand Model to Represent the Viscoplastic Deformation Behavior of Solder Alloys

Journal of Electronic Packaging — Copyright © 2001 by ASME — SEPTEMBER 2001, Vol. 123 / 247

Source: Wang, C. H. (2001). "A Unified Creep–Plasticity Model for Solder Alloys."
**DOI:** 10.1115/1.1371781

- Applies Ar
- Anand's m
- transition t
- Targets so

connectior and its Application to Solder Joints


te at University of Kentucky

9-15 Mon 12:39

## *Constitutive Equations for Hot-Working of Metals*

**Author:** Lallit Anand (1985)

**DOI:** 10.1016/0749-6419(85)90004-X

*One of the foundational papers in thermodynamically consistent viscoplasticity modeling—especially significant in the context of metals subjected to large strains and high temperatures.*

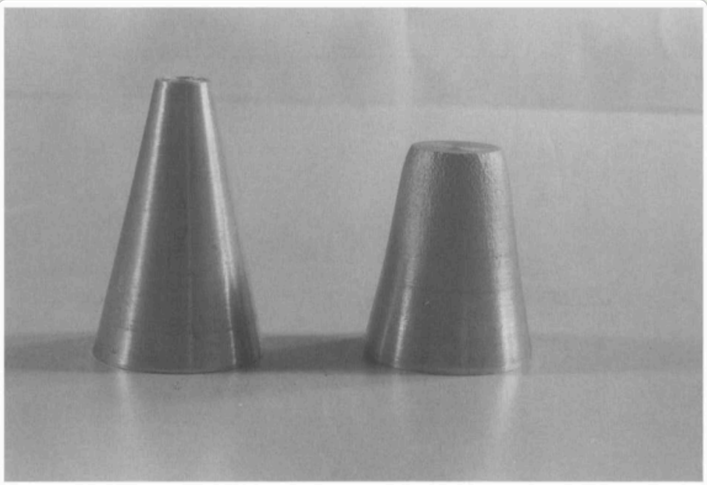

**Fig. 25. 1100 aluminum state gradient specimens before and after testing.**



*International Journal of Plasticity*, Vol. 1, pp. 213-231, 1985
Printed in the U.S.A.

0749-6419/85 $3.00 + .00


# CONSTITUTIVE EQUATIONS FOR HOT-WORKING OF METALS

LALLIT ANAND

Massachusetts Institute of Technology

(Communicated by Theoder Lehmann, Ruhr Universität Bochum)

**Abstract** – Elevated temperature deformation processing – "hot-working," is an important step during the manufacturing of most metal products. Central to any successful analysis of a hot-working process is the use of appropriate rate and temperature-dependent constitutive equations for large, interrupted inelastic deformations, which can faithfully account for strain-hardening, the restoration processes of recovery and recrystallization and strain rate and temperature history effects. In this paper we develop a set of phenomenological, internal variable type constitutive equations describing the elevated temperature deformation of metals. We use a scalar and a symmetric, traceless, second-order tensor as internal variables which, in an average sense, represent an isotropic and an anisotropic resistance to plastic flow offered by the internal state of the material. In this theory, we consider small elastic stretches but large plastic deformations (within the limits of texturing) of isotropic materials. Special cases (within the constitutive framework developed here) which should be suitable for analyzing hot-working processes are indicated.

## I. INTRODUCTION

Hot-working is an important processing step during the manufacture of approximately more than eighty-five percent of all metal products. The main features of hot-working are that metals are deformed into the desired shapes at temperatures in the range of ~0.5 through ~0.9 $\theta_m$, where $\theta_m$ is the melting temperature in degrees Kelvin, and at strain rates in the range of ~$10^{-4}$ through ~$10^3$/sec. It is to be noted that most hot-working processes are more than mere shape-making operations; an important goal of hot-working is to subject the workpiece to appropriate thermo-mechanical processing histories which will produce microstructures that optimize the mechanical properties of the product.

The major quantities of metals and alloys are hot-worked under interrupted non-isothermal conditions. The principles of the physical metallurgy of such deformation processing are now well recognized, e.g., JONAS *et al.* [1969], SELLARS & MCG TEGART [1972], MCQUEEN & JONAS [1975], and SELLARS [1978]. During a deformation pass, the stress is found to be a strong function of the strain rate, temperature, and the defect and microstructural state of the material. The strain-hardening produced by the deformation tends to be counteracted by dynamic recovery processes. These recovery processes result in a rearrangement and annihilation of dislocations in such a manner that as the strain in a pass increases, the dislocations tend to arrange themselves into sub-grain walls. In some metals and alloys (especially those with a high stacking fault energy, e.g., Al, $\alpha$-Fe and other ferritic alloys) dynamic recovery can balance strain-hardening and an apparent steady state stress level can be achieved and maintained to large strains before fracture occurs. In other metals and alloys in which recovery is less rapid (especially those metals with low stacking fault energies, e.g., Ni, $\gamma$-Fe and other austenitic

213

## Kinematics in the Relaxed Configuration

- Elastic deformation gradient:

$$F = F^e F^p \quad \Rightarrow \quad F^e = F F^{p-1}$$

- Elastic right Cauchy-Green tensor:

$$C^e = F^{eT} F^e$$

- Elastic Green–Lagrange strain tensor:

$$E^e = \frac{1}{2}(C^e - I)$$

**Sum**

- Elastic kinematics and stress measures are formulate
plastic and elastic contributions.
- Stress Power Split allows Anand to cleanly isolate pla
- Green-Lagrange strain tensor $E^e$ is used because it
relaxed configuration
- The right Cauchy-Green tensor $C^e = F^{e^T} F^e$ is requi
deformation gradient $F^e$ without referencing spatial c





**Numerical Values**

- $S_0 = 5.633 \times 10^7$ Pa
- $Q/R = 10830$ K
- $A = 1.49 \times 10^7$ s$^{-1}$
- $\xi = 11$
- $m = 0.303$
- $h_0 = 2.6408 \times 10^9$ Pa
- $\hat{s} = 8.042 \times 10^7$ Pa
- $n = 0.0231$
- $a = 1.34$

These constants match Wang's paper for modeling 60Sn40Pb viscoplasticity.

## Forward Euler Explicit time ir

### Initialization

- Material constants: $A, Q/R, j, m, h_0, \hat{s}, n, a, E$
- Strain rate: $\dot{\varepsilon}$
- Temperature set: $\{T_i\}$
- Set: $\varepsilon^p(0) = 0, \quad s(0) = \hat{s}$

### Time Evolution Loop

1. $\varepsilon_{\text{total}}(t) = \dot{\varepsilon}\, t$
2. $\sigma_{\text{trial}} = E(\varepsilon_{\text{total}} - \varepsilon^p)$
3. Compute $x = \frac{j\sigma}{s}$
4. Approximate $\sinh(x)$ (linearize if $|x| \ll 1$)
5. $\dot{\varepsilon}^p = Ae^{-Q/RT}(\sinh(x))^{1/m}$



## iate) Configuration

### What Happens in the Relaxed Configuration?

- The elastic deformation gradient $F^e$ is measured from the relaxed state to the current deformed state.
- Elastic strain measures like $C^e$ and $E^e$ are defined in this configuration.
- The Kirchhoff stress $\tilde{\mathbf{T}}$ is naturally associated with the relaxed volume.
- Plastic flow is accounted for separately through the plastic velocity gradient $\mathbf{L}^p$.

---

**mary:**

cleanly, enabling proper definition of thermodynamics and

Relaxed (Intermed

## Context for the Relaxed Configuration

- The relaxed configuration represents the material after removing plastic deformations but before applying new elastic deformations.
- It is introduced to separate permanent plastic effects from recoverable elastic effects.
- All thermodynamic potentials, internal variables, and evolution laws are defined relative to this frame.
- The relaxed state provides a clean, natural reference for measuring elastic strain $E^e$ and computing dissipation.

---

**Sum**

- The relaxed configuration isolates elastic responses
plastic evolution laws.



ıtegration scheme Pseudocode

### Plastic Flow & Resistance Evolution

6. $s^* = \hat{s}\left(\frac{\dot{\varepsilon}^p}{A}e^{Q/RT}\right)^n$
7. $\dot{s} = h_0\left|1 - \frac{s}{s^*}\right|^a \mathrm{sign}\left(1 - \frac{s}{s^*}\right)\dot{\varepsilon}^p$
8. Update: $\varepsilon^p(t+\Delta t) = \varepsilon^p(t) + \dot{\varepsilon}^p \Delta t$
9. Update: $s(t+\Delta t) = s(t) + \dot{s}\Delta t$
10. Record $(\varepsilon_{\mathrm{total}}, \sigma_{\mathrm{trial}})$

### Termination

- Stop when $\varepsilon_{\mathrm{total}} \geq \varepsilon_{\max}$
- Plot $\sigma$ vs $\varepsilon$ for all $T_i$

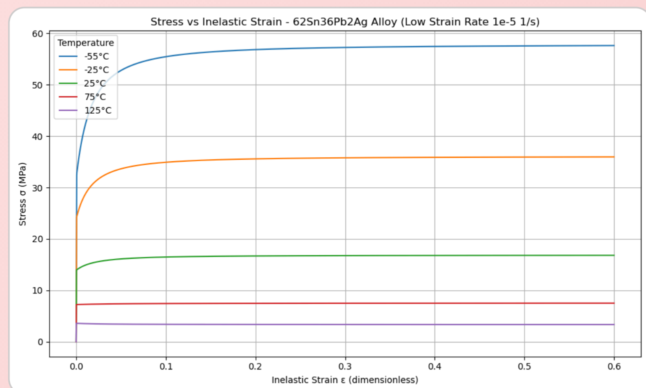

ıd Thermal Effects

Forward Euler Schei

```
import numpy as np
import matplotlib.pyplot as plt
from scipy.integrate import solve_ivp

# Material constants for 62Sn36Pb2Ag solder alloy
A = 2.24e8          # 1/s
Q_R = 11200         # K
j = 13              # dimensionless
m = 0.21            # dimensionless
h0 = 1.62e10        # Pa
s0 = 8.47e7         # Pa
s_hat = 8.47e7      # Pa
n = 0.0277          # dimensionless
a = 1.7             # dimensionless
E = 5.2e10          # Pa (Elastic modulus)

# Temperatures in Kelvin
T_C = [-55, -25, 25, 75, 125]
T_list = [T + 273.15 for T in T_C]

# Simulation parameters
strain_rate = 1e-5  # 1/s
eps_total_max = 0.6
t_max = eps_total_max / strain_rate
time_steps = 10000
t_eval = np.linspace(0, t_max, time_steps)

# Define the ODE system
def system(t, y, T):
    ep_p, s = y
    eps_total = strain_rate * t
    sigma_trial = E * (eps_total - ep_p)
    x = j * sigma_trial / s

    if np.abs(x) < 0.01:
        sinh_x = x
    else:
        sinh_x = np.sinh(np.clip(x, -30, 30))

    sinh_x = np.maximum(sinh_x, 1e-12)
    dep_p = A * np.exp(-Q_R / T) * sinh_x**(1/m)

    s_star = s_hat * (dep_p / A * np.exp(Q_R / T))**n
    ds = h0 * np.abs(1 - s/s_star)**a * np.sign(1 - s/s_star) * dep_p

    return [dep_p, ds]

# Plotting
```

## Why Subtract the Thermal Term?

- Thermal expansion creates strain even without external forces.
- Without subtracting $\mathbf{\Pi}\dot{\theta}$, the model would falsely attribute thermal strain as mechanical stress.
- Subtracting isolates the true mechanical response from thermal effects.

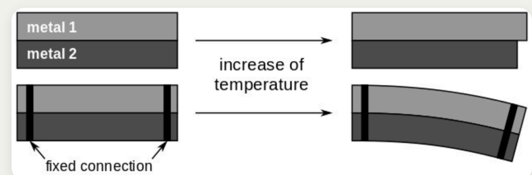


ɾain without force.
ɲechanical strains generate stresses.
del physically accurate during heating and cooling.

## Stress Evolution and Thermal Effects



In the stress evolution equation,

$$\overset{\nabla}{\mathbf{T}} = \mathbb{L}\left[\mathbf{D} - \mathbf{D}^p\right] - \mathbf{\Pi}\dot{\theta},$$

the term $\mathbf{\Pi}\dot{\theta}$ represents the stress change that would occur due to pure thermal expansion alone, without any mechanical loading.

**Summary:**

- Thermal expansion induces st
- Subtracting $\mathbf{\Pi}\dot{\theta}$ ensures only r
- This keeps the constitutive mo

Strain rate sensit

- As $m \to 0$, rate insensitive
- As $m \to 1$, small stress ch

ion for the Stress

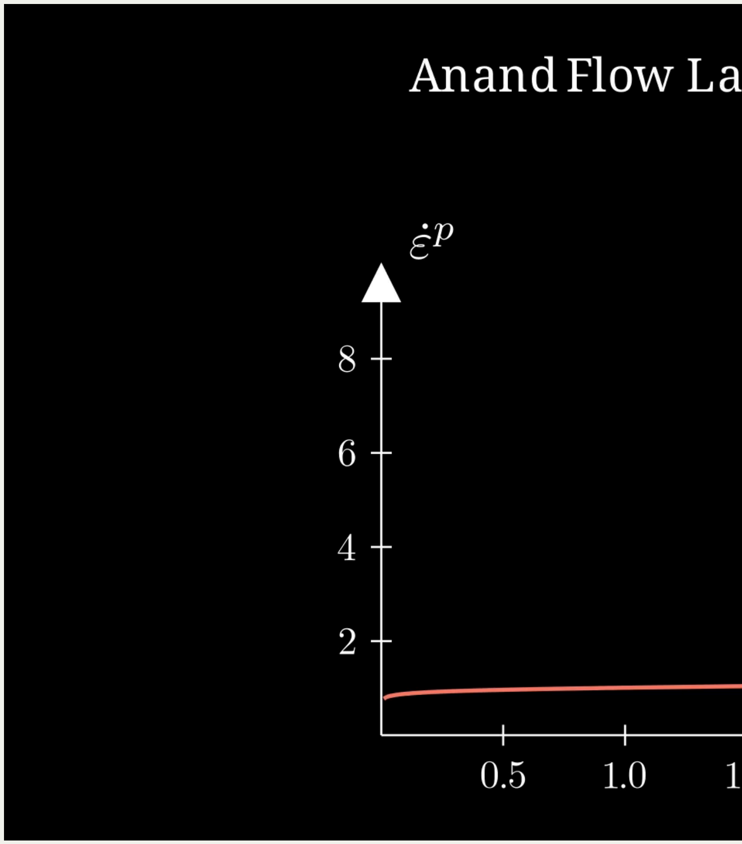


Material Tensors and Operators

- $\mathbb{L} = 2\mu\mathbf{I} + \left(\kappa - \frac{2}{3}\mu\right) \mathbf{1} \otimes \mathbf{1}$ — isotropic elasticity tensor
- $\mathbb{L}\mathbf{D}$ represents how instantaneous strain rates generate stresses according to the elastic material's stiffness properties.
- $\mu = \mu(\theta)$, $\kappa = \kappa(\theta)$ — temperature-dependent moduli
- $\mathbf{\Pi} = (3\alpha\kappa)\mathbf{1}$ — stress-temperature coupling
- $\alpha = \alpha(\theta)$ — thermal expansion coefficient
- $\mathbf{D} = \mathrm{sym}(\nabla\mathbf{v})$ — stretching tensor
- $\mathbf{W} = \mathrm{skew}(\nabla\mathbf{v})$ — spin tensor
- $\mathbf{I}$ = fourth-order identity tensor
- $\mathbf{1}$ = second-order identity tensor

nann derivative to ensure frame indifference.
ed by isotropic fourth-order tensor $\mathbb{L}$.
oduces additional stress through $\mathbf{\Pi}\dot{\theta}$.

:ivity of stress m

Evolution Equati: (yield)
ange causes big change in strain rate

Stress Evolution Equation (Rate form of Hooke's Law)

$$\overset{\triangledown}{\mathbf{T}} = \mathbb{L}\left[\mathbf{D} - \mathbf{D}^p\right] - \mathbf{\Pi}\dot{\theta}$$

(rate-form Hooke's law for finite deformation plasticity, with frame-indifference enforced through the Jaumann rate.)

Jaumann Rate Definition

$$\overset{\triangledown}{\mathbf{T}} = \dot{\mathbf{T}} - \mathbf{WT} + \mathbf{TW}$$

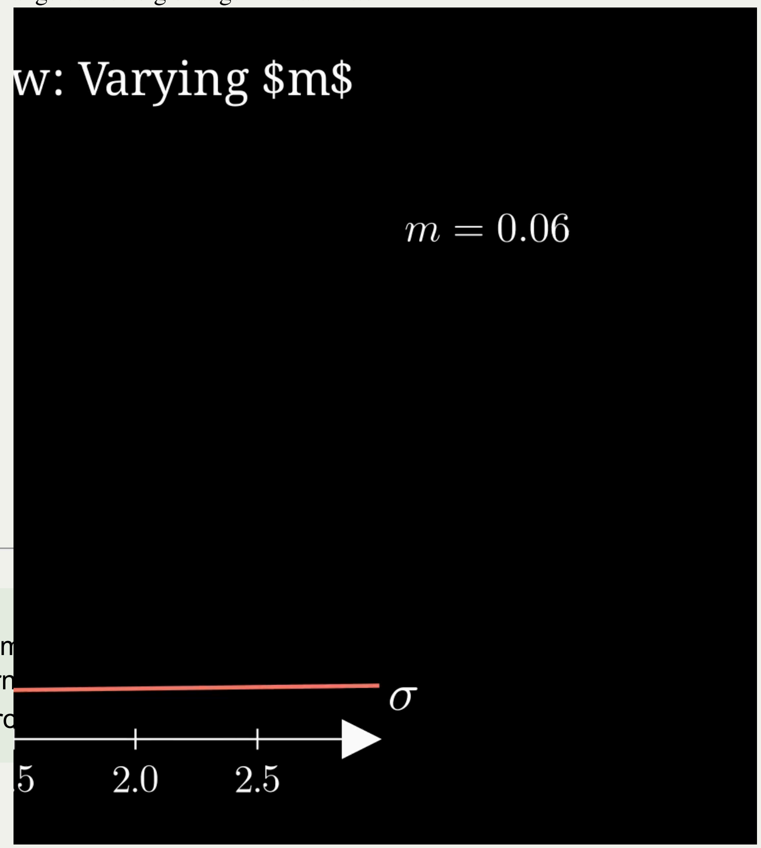


**Summary:**
- Stress rate follows Jaum
- Elastic response govern
- Thermal expansion intro

## Flow rule

### Tensorial Flow Rule (directional form)

$$\mathbf{D}^p = \dot{\epsilon}^p \left( \frac{3}{2} \frac{\mathbf{T}'}{\bar{\sigma}} \right)$$

### Equivalent Stress Definition

$$\bar{\sigma} = \sqrt{\frac{3}{2} \mathbf{T}' : \mathbf{T}'}$$

### Plastic Strain Rate (magnitude form)

$$\dot{\epsilon}^p = A \exp\left( -\frac{Q}{R\theta} \right) \left[ \sinh\left( \xi \frac{\bar{\sigma}}{s} \right) \right]^{1/m}$$

### Full Flow Rule with Hyperbolic Sine

$$\mathbf{D}^p = A \exp\left( -\frac{Q}{R\theta} \right) \left[ \sinh\left( \xi \frac{\bar{\sigma}}{s} \right) \right]^{1/m} \left( \frac{3}{2} \frac{\mathbf{T}'}{\bar{\sigma}} \right),$$

$$= \dot{\gamma}^p \left( \frac{\widetilde{\mathbf{T}}'}{2\bar{\tau}} \right), \quad \bar{\tau} = \left\{ \frac{1}{2} \mathrm{tr}(\widetilde{\mathbf{T}}'^2) \right\}^{1/2}$$

**Summary:**

- Direction given by $\mathbf{T}'$.
- Magnitude determined by hyperbolic sine based on $\bar{\sigma}/s$.
- $\bar{\tau}$ represents the effective shear stress computed from deviatoric stress.
- $\bar{\sigma} = \sqrt{\frac{3}{2}\mathbf{T}' : \mathbf{T}'}$ is the von Mises Equivalent stress, but is formally defined without yield point
- Full flow = **direction** × **magnitude**.

pipe = Pipe(); creates a Pipe Class. As the functio

1. obj.CaseId - stores properties like Re, rotation number $S$, experiment frequently called vectors (rMat $r = 1, \ldots, 0.5$)
2. obj.pod - eigen data, used for calculating POD
3. obj.solution - computed POD modes
4. obj.plt - plot configuration





## Stress and Power Quantities

- Kirchhoff stress (weighted Cauchy stress):

$$\widetilde{\mathbf{T}} = (\det F)\mathbf{T}$$

- Stress power split:

$$\dot{\omega} = \dot{\omega}^e + \dot{\omega}^p$$

$$\dot{\omega}^e = \widetilde{\mathbf{T}} : \dot{E}^e \quad , \quad \dot{\omega}^p = (C^e\widetilde{\mathbf{T}}) : \mathbf{L}^p$$

---

**mary:**

ed relative to the relaxed configuration, cleanly separating

astic dissipation from elastic storage.
symmetrically captures nonlinear elastic strain relative to the

red as an intermediate to compute $E^e$ from the elastic
coordinates

Dissipation Separation: Elasti

### Thermodynamic Separation

1. **Start with Total Dissipation:**

$$\mathcal{D} = \dot{\omega} - \dot{\psi} \geq 0$$

where $\dot{\omega} = \widehat{\mathbf{T}} : \dot{\mathbf{E}}^e + (\mathbf{C}^e\widehat{\mathbf{T}}) : \mathbf{L}^p$

2. **Split Stress Power:**

$$\dot{\omega} = \dot{\omega}^e + \dot{\omega}^p$$

with:

- $\dot{\omega}^e = \widehat{\mathbf{T}} : \dot{\mathbf{E}}^e$
- $\dot{\omega}^p = (\mathbf{C}^e\widehat{\mathbf{T}}) : \mathbf{L}^p$

3. **Group Terms with $\dot{\psi}$:**

$$(\dot{\omega}^e - \dot{\psi}) + \dot{\omega}^p \geq 0$$

4. **Apply Elastic Energy Consistency:**

$$\dot{\omega}^e - \dot{\psi} = 0 \quad \Rightarrow \quad \dot{\omega}^p \geq 0$$



ıyout 2

ggf betwen $\alpha\Phi$) according to Papers (Citriniti George 2000 for Classic POD,

dial graph)

Key Physical Insights

- **Elastic deformations** are recoverable and do not cause entropy production.
- **All dissipation** stems from the plastic flow: $\dot{\omega}^p$.
- **Plastic work** increases entropy and governs viscoplastic evolution.

**Summary:**
The stress power split ensures that the second law is satisfied by assigning dissipation solely to irreversible processes.





1. ↪ initPod.m
   - carries out POD calculations (quadrature, multiplication
     Hellstrom Smits 2017 for Snapshot POD)
2. ↪ timeReconstructFlow.m
   - performs 2d reconstruction + plotSkmr (generates 1d ra

Reference C

## Framework in the Reference Configuration

- The free energy $\psi$ is defined relative to the reference configuration.
- State variables like $E^e, \theta, \bar{g}, \bar{\mathbf{B}}, s$ are used as arguments of $\psi$.
- Stress is expressed using the second Piola–Kirchhoff tensor $\mathbf{S}$.
- Dissipation inequality, stress–strain relations, and evolution laws are all written in reference variables.
- Mass density $\rho_0$ from the reference configuration normalizes all terms.

**Sum**

- In the reference configuration, all energy storage, str
with reference-frame quantities for consistency and c



.ayout

in binary files, takes eg m-fft

corrMat, finds eigenvalues

1.1. L

1. b7.m
2. initSpectral.m
   - reads i
3. ↪ initEigs.m
   - forms



'onfiguration

## Key Equations in the Reference Frame

- Free energy:

$$\boxed{\psi = \psi(E^e, \theta, \bar{g}, \bar{\mathbf{B}}, s)}$$

- Dissipation inequality:

$$\boxed{\dot{\psi} + \eta\dot{\theta} - \rho_0^{-1}\mathbf{S} : \dot{E} + (\rho_0\theta)^{-1}\mathbf{q}_0 \cdot \mathbf{g}_0 \leq 0}$$

- Constitutive relation:

$$\boxed{\mathbf{S} = \rho_0 \frac{\partial \psi}{\partial E^e}}$$

**mary:**

ess updates, and internal variable evolution are formulated
bjectivity.

## Thermodynamic Quantities

- Free energy density:

$$\boxed{\psi = \epsilon - \theta\eta}$$

- Reduced dissipation inequality:

$$\boxed{\dot{\psi} + \eta\dot{\theta} - \rho^{-1}\mathbf{T} : \mathbf{L} + (\rho\theta)^{-1}\mathbf{q} \cdot \mathbf{g} \leq 0}$$

- State variables:

$$\{E^e, \theta, \bar{g}, \bar{\mathbf{B}}, s\}$$

with $E^e$ as elastic strain and $s$ as internal resistance.



**Summary:**

- Free energy and dissipatio
- Stress power naturally split
- Kirchhoff stress simplifies s

1. Code Execut

## Stress Power and Kirchhoff Stress

- Stress power per relaxed volume:

$$\boxed{\dot{\omega} = \left(\frac{\rho_0}{\rho}\right) \mathbf{T} : \mathbf{L}}$$

- Weighted Cauchy (Kirchhoff) stress:

$$\boxed{\widetilde{\mathbf{T}} = (\det F)\mathbf{T}} \quad \text{or} \quad \boxed{\widetilde{\mathbf{T}} = \left(\frac{\rho_0}{\rho}\right) \mathbf{T}}$$

- Decomposition of stress power:

$$\boxed{\dot{\omega} = \dot{\omega}^e + \dot{\omega}^p}$$

$$\dot{\omega}^e = \widetilde{\mathbf{T}} : \dot{E}^e, \quad \dot{\omega}^p = (C^e \widetilde{\mathbf{T}}) : \mathbf{L}^p$$

---

n govern thermodynamic consistency.
s into elastic and plastic parts.
tress evolution accounting for volume changes.

# POD Analysis of Turbulent Pipe Flow

M. Raba

Created: 2025-09-15 Mon 12:39

Exchange the order of summation anc

$$\sum_l \Phi_{\mathrm{T}}^{(l)}(k;m;r)\left(\frac{1}{\tau}\int_0^\tau \alpha^{(}\right.$$

ınt Switches

Due to the orthogonality, namely tıns (above) are called, data is stored in sub-structs:

$\langle a^{(n)}\alpha^{(p)}\rangle$ :al flags such as quadrature (simpson/trapezoidal), number of gridpoints,

all terms where $l \neq n$ will vanish, an

$$\Phi_{\mathrm{T}}^{(n)}(k;m;r)\left(\frac{1}{\tau}\int_0^\tau \alpha^{(n)}\right.$$

This derivation assumes the normalization of modes and their orthogonality, form that reveals the spatial structure ( $\Phi_{\mathrm{T}}^{(n)}$ ) (

## 2. Equations Used

ivation

uation, consider the integral:

$$t)\alpha^{(n)^*}(k;m;t)dt.$$

ith its expansion:

$$(k;m;t)\Big)\,\alpha^{(n)^*}(k;m;t)dt.$$

3. Der

To derive the questioned equ

$$\frac{1}{\tau}\int_0^{\tau} \mathbf{u}_{\mathrm{T}}(k;m;r,$$ in Code Procedure

Substitute $\mathbf{u}_{\mathrm{T}}$ w

$$\frac{1}{\tau}\int_0^{\tau} \left(\sum_l \Phi_{\mathrm{T}}^{(l)}(k;m;r)\alpha^{(l}\right.$$

The following equations a

nstruction

$$\int_{r'} \mathbf{S}\left(k;m;r,r'\right)\Phi^{(n)}\left(k;m;r'\right)$$

his is incorrect. The necessary use of (factor $\gamma$) is incorrect

$$\mathbf{S}\left(k;m;r,r'\right) = \lim_{\tau\to\infty}\frac{1}{\tau}\int_0^{\tau}\mathbf{u}(k$$

$$\alpha^{(n)}(k;m;t) = \int_r \mathbf{u}(k;m;r,t)$$

re used in the above code.

2.5. Reco

$$r' \mathrm{d}r' = \lambda^{(n)}(k;m)\Phi^{(n)}(k;m;r)$$

In order to reconstruct in code, caseId.fluctuation = 'off'. T

$$;m;r,t)\mathbf{u}^*(k;m;r',t)\,\mathrm{d}t$$

$$^{(n)^*}(k;m;r)r\,\mathrm{d}r$$

tion is given by

$$\int_{r'} \underbrace{r^{1/2} S_{i,j}\left(r, r'; m; f\right) r'^{1}}_{W_{i,j}(r,r';m;f)} \Rightarrow$$

$$= \underbrace{\lambda^{(n)}(m,f)}_{\hat{\lambda}^{(n)}(m;f)} \underbrace{r^{1/2}\phi_i^{(n)}(r;}_{\hat{\phi}_i^{(n)}(r,m;} \sum_{n=1} \sum_{m=0} \alpha^{(n)}(m;t)\Phi^{(n)}(r;m;x)$$

construction can only be recovered by writing for $\text{factor} \gg 0$.

$$\alpha_n(m;t) = \int_r \mathbf{u}(m;r,t)$$

$$\gamma) \sum_{n=1} \sum_{m=0} \alpha^{(n)}(m;t)\Phi^{(n)}(r;m;x)$$

2.4. Reco Equations (Fixed)

The reconstruc

$$q(\xi,t) - \bar{q}(\xi) \approx \sum_{j=1}^{r} a_j(t)\varphi_j(\xi) \quad {}^{1/2}\underbrace{\phi_j^{*(n)}(r';m;f)\, r'^{1/2}\,\mathrm{d}r'}_{\hat{\phi}_j^{\psi(i)}(r';m;f)}$$

$$q(r,\theta,t;x) = \bar{q}(r,\theta,t;x) + \underbrace{m;f)}_{}$$

$f)$

Since the snapshot pod implementation is not error-free, the re $^{1/2}\Phi_n^*(m;r)dr$

$$q(r,\theta,t;x) = \bar{q}(r,\theta,t;x) + (\text{factor}$$

## 2.3. Snapshot POD Equations

$$\lim_{\tau\to\infty}\frac{1}{\tau}\int_0^{\tau}\mathbf{u}_{\mathrm{T}}(k;m;r,t)\alpha^{(n)^*}(k;m;t)\mathrm{d}t$$
$$=\Phi_{\mathrm{T}}^{(n)}(k;m;r)\lambda^{(n)}(k;m)$$
$$\mathbf{R}\,(k;m;t,t')=\int_r\mathbf{u}(k;m;r,t)\mathbf{u}^*\,(k;m;r,t')\,r\,\mathrm{d}r$$
$$\lim_{\tau\to\infty}\frac{1}{\tau}\int_0^{\tau}\mathbf{u}_{\mathbf{T}}(k;m;r,t)\alpha^{(n)*}(k;m;t)\,\mathrm{d}t$$
$$=\Phi_{\mathbf{T}}^{(n)}(k;m;r)\lambda^{(n)}(k;m).$$

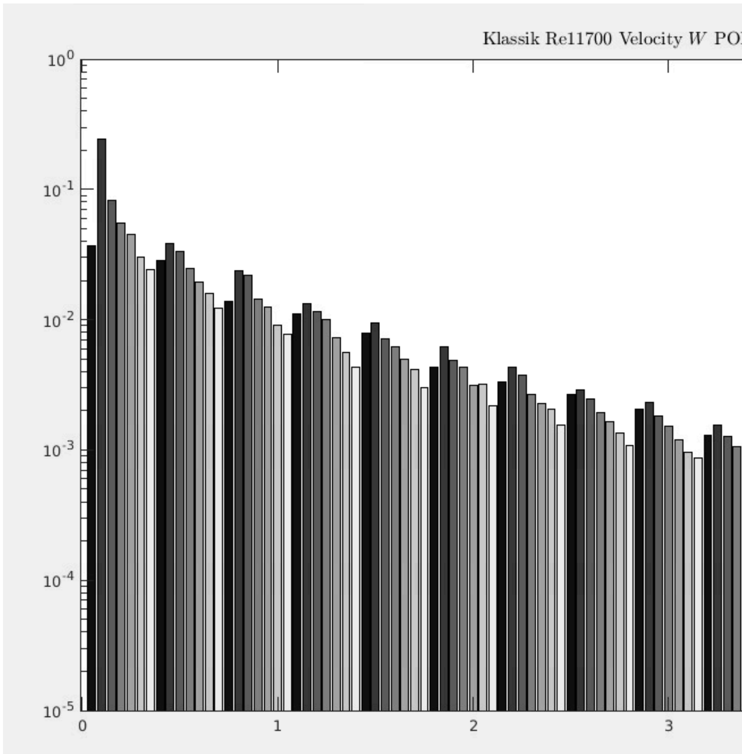


erivation

l integration, and apply orthogonality,

$$ {}^{l)}(k;m;t)\alpha^{(n)^*}(k;m;t)dt\Big) . $$

hat $\alpha^{(n)}$ and $\alpha^{(p)}$ are uncorrelated

$$ = \lambda^{(n)}\delta_{np} $$

d there remains only the $l = n$ term,

$$ (k;m;t)\alpha^{(n)^*}(k;m;t)dt\Big) . $$

along with the eigenvalue relationship to simplify the original integral into a of each mode scaled by its significance $\left(\lambda^{(n)}\right)$.

ı=0 Classic

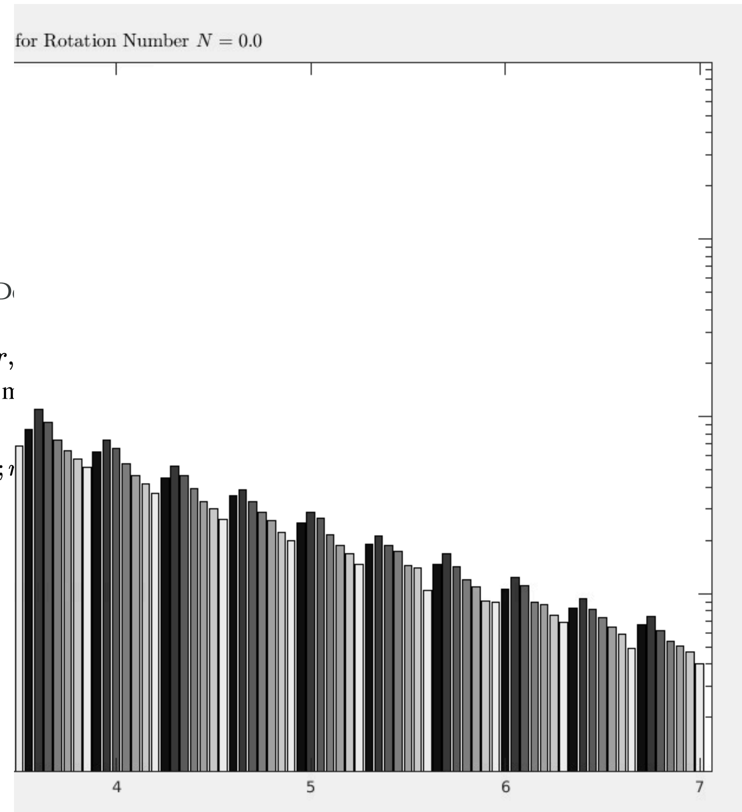


3.2. 6 D

The cross-correlation tensor $\mathbf{R}$ is defined as $\mathbf{R}\,(k; m; t, t') = \int_r \mathbf{u}(k; m; r,$
$[t \times t']$ tensor. The $n$ POD n

$$\lim_{\tau\to\infty} \frac{1}{\tau} \int_0^{\tau} \mathbf{u}_{\mathrm{T}}(k; m; r, t)\alpha^{(n)^*}(k;$$

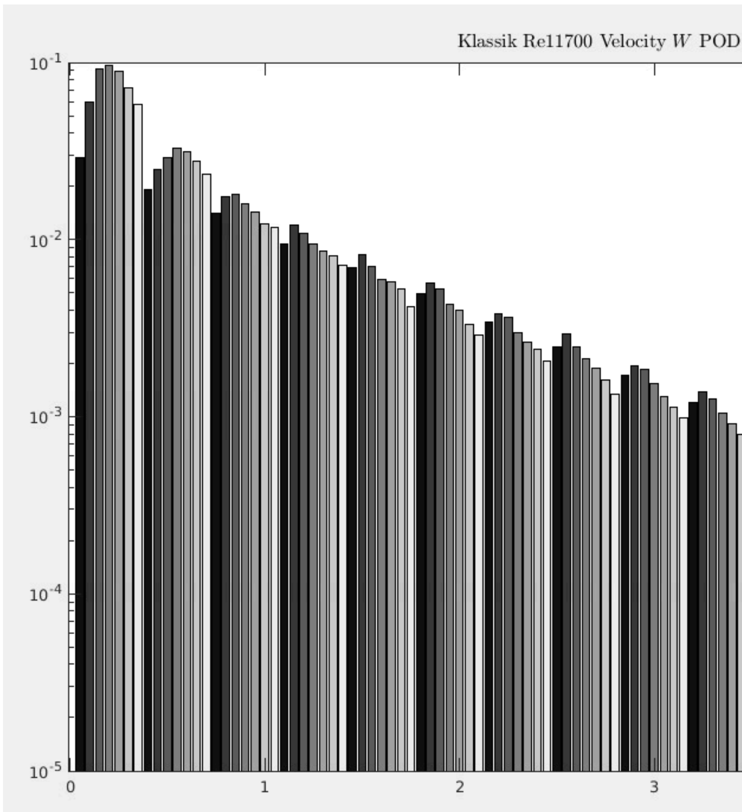


erivation

$t)\mathbf{u}^*(k;m;r,t')\,r\,\mathrm{d}r$. This tensor is now transformed from $[3r \times 3r']$ to a
nodes are then constructed as,

$$n;t)\mathrm{d}t = \Phi_{\mathrm{T}}^{(n)}(k;m;r)\lambda^{(n)}(k;m).$$

POD S=3.0

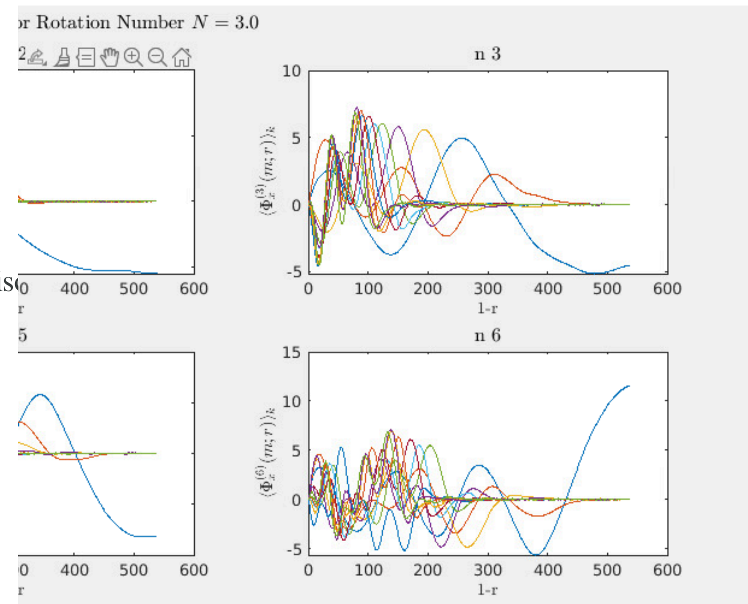


4. Result Comparis

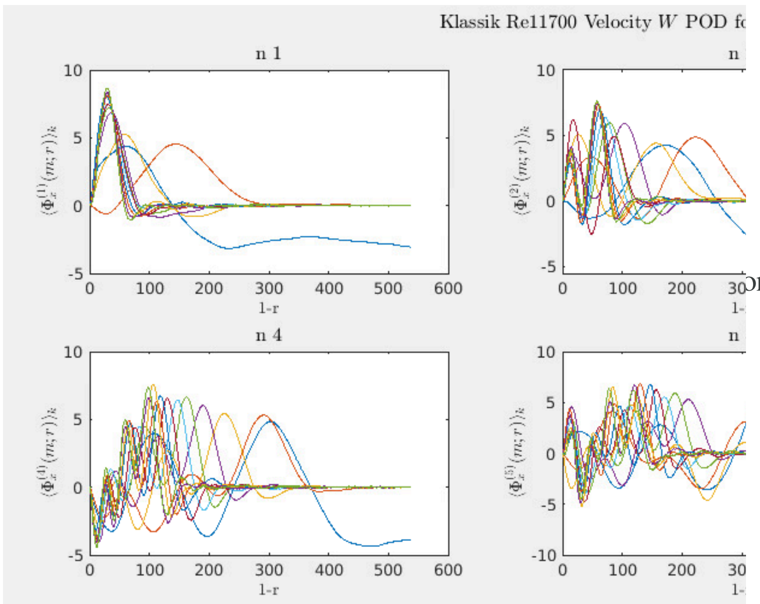


on Classic/Snapshot

4.1. Radi POD S=0.0

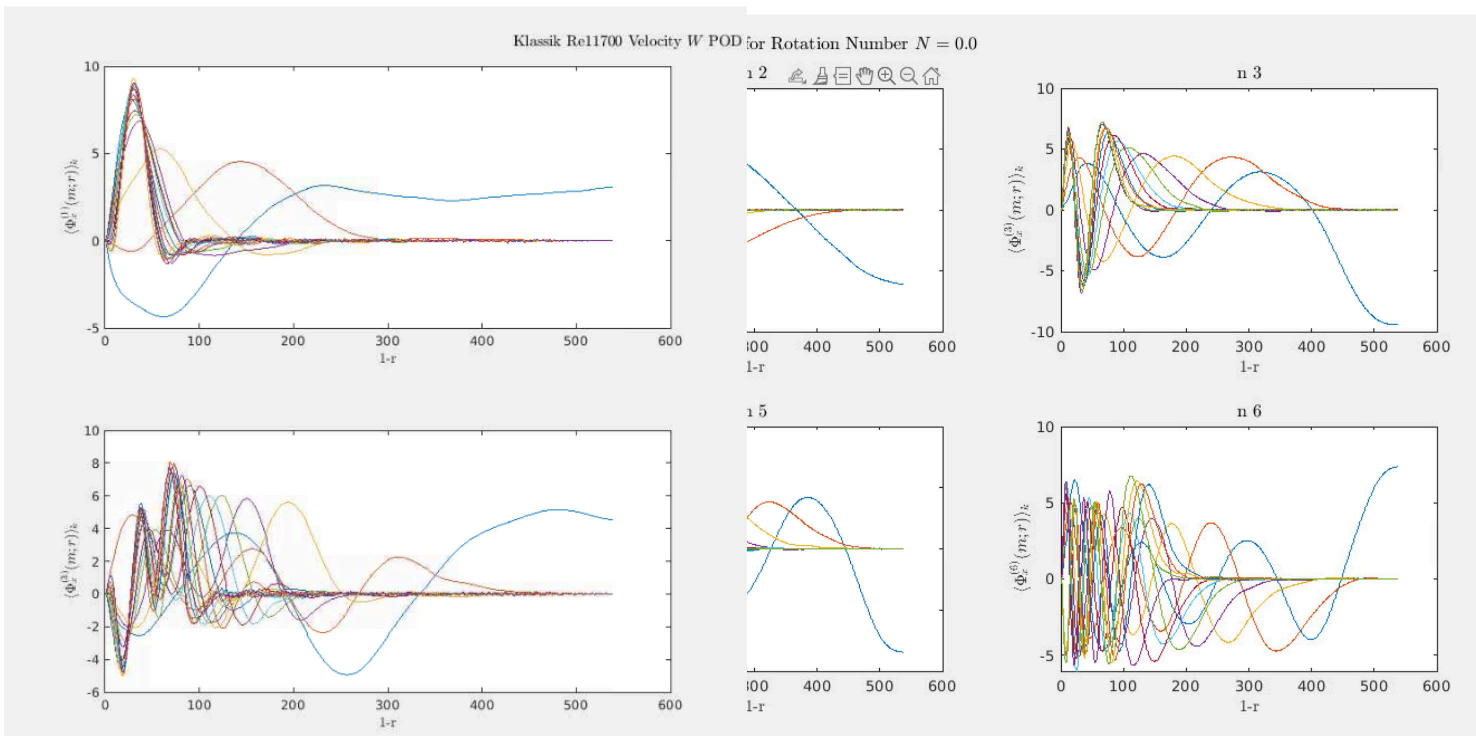

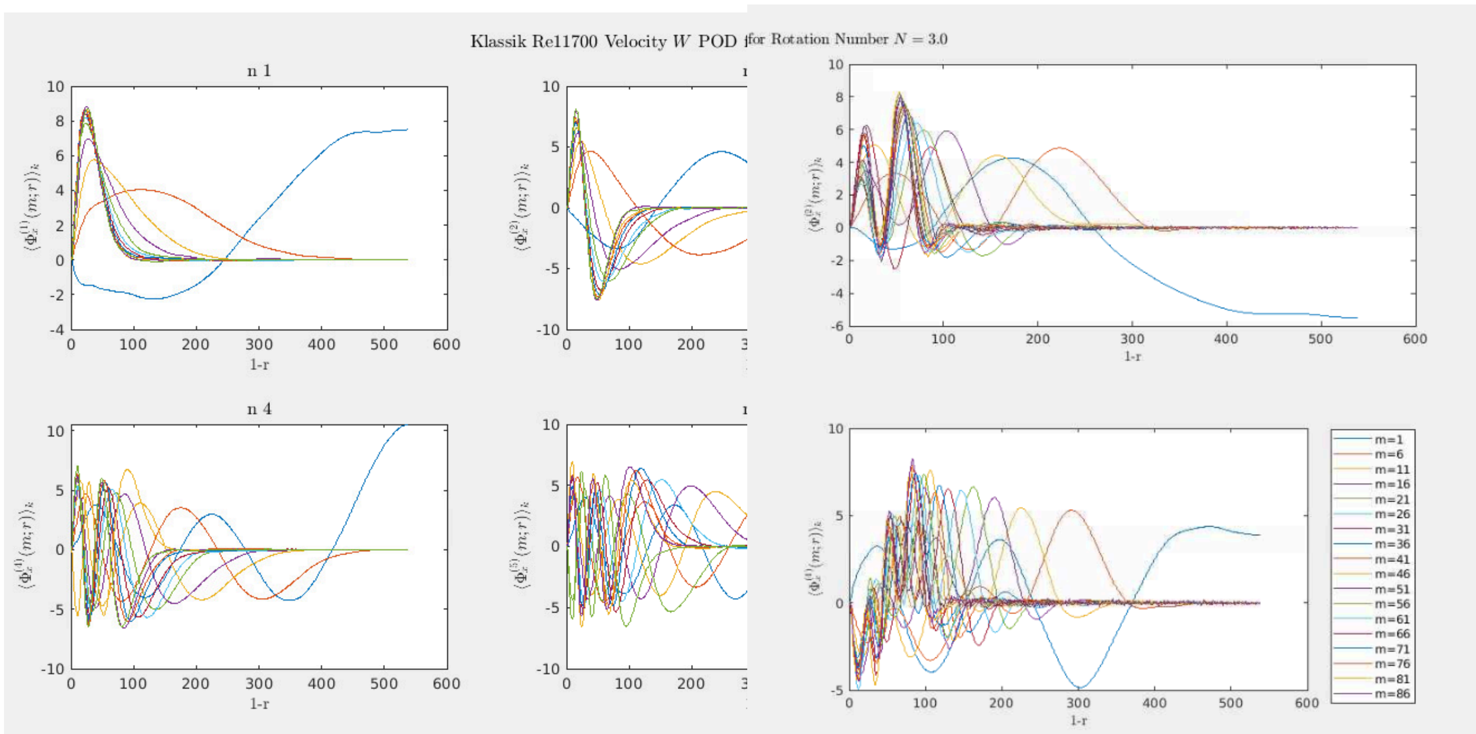
Klassik Re11700 Velocity $W$ POD for Rotation Number $N = 3.0$
n 1
n 4
1-r
m=1
m=6
m=11
m=16
m=21
m=26
m=31
m=36
m=41
m=46
m=51
m=56
m=61
m=66
m=71
m=76
m=81
m=86

## 4.2. Snapshot-Classic Comparison

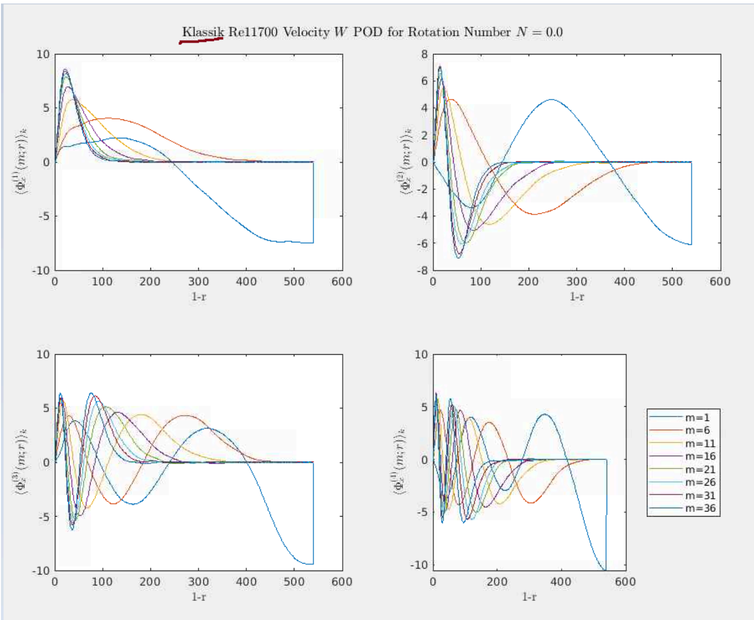


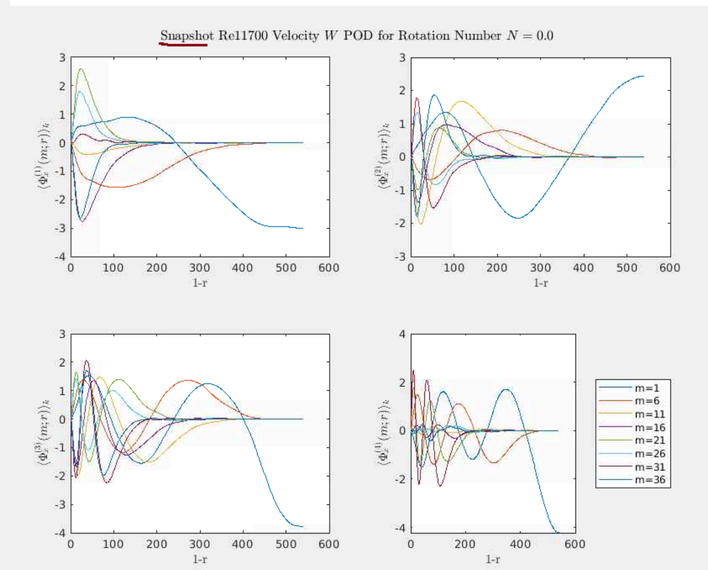

; Classic

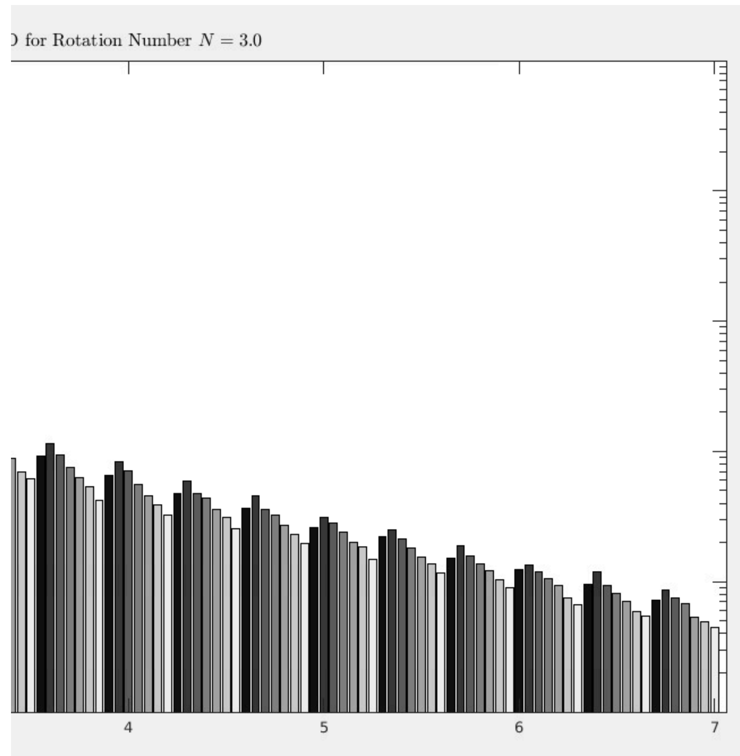

5.2. A

nalysis

# 6. Recon

struction

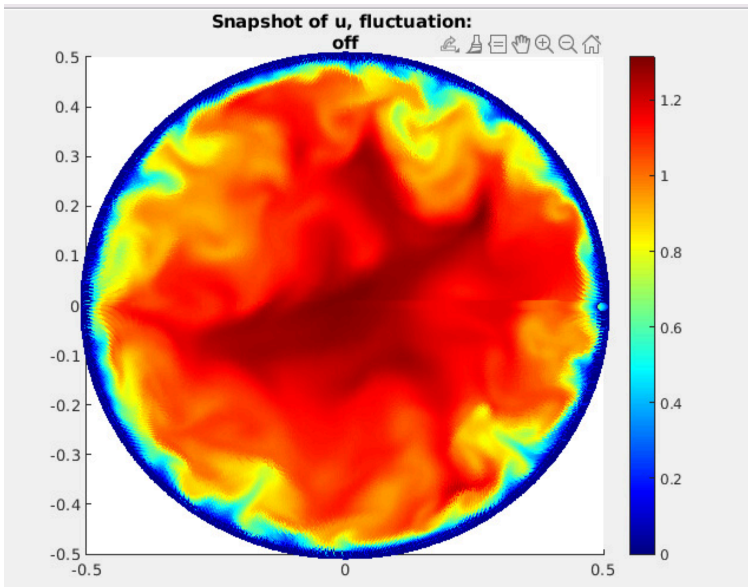
Snapshot of u, fluctuation:
off
0.5
0.4
0.3
0.2
0.1
0
-0.1
-0.2
-0.3
-0.4
-0.5
-0.5
0
0.5
1.2
1
0.8
0.6
0.4
0.2
0

nstruction

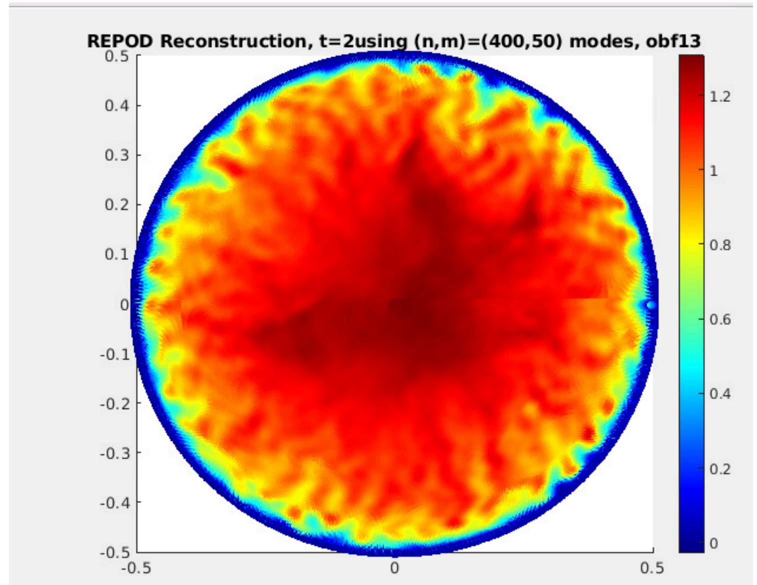

REPOD Reconstruction, t=2using (n,m)=(400,50) modes, obf13
0.5
0.4
0.3
0.2
0.1
0
-0.1
-0.2
-0.3
-0.4
-0.5
-0.5
0
0.5
1.2
1
0.8
0.6
0.4
0.2
0